5-2020

Selfsame Epoxide-Amine Microparticle Systems: Investigation of Crosslink Density

John J. Peyrefitte

The University of Southern Mississippi

Selfsame Epoxide-Amine Microparticle Systems: Investigation of Crosslink Density

by

John J. Peyrefitte

A Thesis
Submitted to the Honors College of
The University of Southern Mississippi
in Partial Fulfillment
of Honors Requirements

May 2020

Approved by:

_____

Jeffrey S. Wiggins, Ph.D., Thesis Adviser
Professor of Polymer Science and Engineering

_____

Derek L. Patton, Ph.D., Director
School of Polymer Science and Engineering

_____

Ellen Weinauer, Ph.D., Dean
Honors College

Abstract

Epoxide-amine matrix materials containing microparticles with the same chemical composition provide a model system to study interphase formation in highly crosslinked epoxide-amine matrix materials. The epoxide monomer was varied between three different monomer systems to study the model system's relationship with crosslink density. The same amine monomer, cure procedure, and stoichiometric ratio of epoxide and amine groups were used to prepare each type of microparticle and matrix material. The differences in the epoxide monomer structure affected the crosslink density of the unmodified matrix material, which was concluded to influence the effect of microparticle presence on crosslink density. For the unmodified matrix material with the lowest crosslink density, the introduction of microparticles led to the greatest increase in crosslink density. The differences in the epoxide monomer structure also affected network formation upon particle incorporation. Specifically, the presence of tertiary amines in the epoxide monomer structure was related to the effect of microparticle presence on network homogeneity. For the epoxide monomers with less tertiary amines, the network homogeneity was decreased upon microparticle incorporation. An adequately high presence of tertiary amines in the epoxide monomer structure was concluded to prevent the formation of a poor interphase.

Keywords: Selfsame, epoxide-amine, microparticles, crosslink density

Dedication

To my family, friends, and anybody who has ever inspired me.

Acknowledgments

I would like to thank Dr. Jeffrey S. Wiggins for his support, encouragement, and guidance as my thesis adviser and for giving me the opportunity to work with the Wiggins Research Group. The opportunity to work with the group has become a significant component of my experience at the University of Southern Mississippi, and I am grateful for how it has helped me to grow as a researcher and as a person.

I would like to thank everyone in the Wiggins Research Group for providing encouragement and guidance and for contributing to many enjoyable learning experiences. I especially want to thank Dr. Travis Palmer for being my graduate student mentor. I will always be grateful for your dedication and patience as my mentor and for everything you have taught me. I also want to thank Jared Bates especially for his guidance and encouragement. Thank you all for everything.

Table of Contents

List of Tables

List of Figures

List of Abbreviations

ATR-FTIR	attenuated total reflectance Fourier transform infrared
CFRP	carbon fiber-reinforced polymer
DGEBA	diglycidyl ether of bisphenol-A
DSC	differential scanning calorimetry
DMA	dynamic mechanical analysis
DOC	degree of conversion
EEW	epoxide equivalent weight
FT-NIR	Fourier transform near-infrared
FWHM	full width at half maximum
IPDA	isophorone diamine
PPG	polypropylene glycol
p-TGAP	triglycidyl-p-aminophenol
TGDDM	tetraglycidyl-4,4’-diaminodiphenylmethane
T_g	glass transition temperature
WT%	percent by weight

Chapter 1: Introduction

A fiber-reinforced composite material consists of two main components: the fiber reinforcement and the matrix material. The composite material exhibits properties that are not exhibited by the components individually.[1] In recent years, carbon fiber-reinforced polymer (CFRP) composite materials have become increasingly prominent as structural materials in aerospace applications. In comparison to metals, CFRPs provide a much greater strength-to-weight ratio.[1] Thus, when they are used in place of metals, they can significantly reduce the weight of an aircraft.[1] For aerospace applications, weight reduction provides many benefits, and it serves as a driving force for the implementation of polymer composite materials in aerospace applications. For example, weight reduction decreases fuel requirements for aircraft, which results in lower operating costs and additional space for cargo.[1]

Because CFRP composites will continue to be employed as aerospace structural materials, improving their material properties is a prominent research focus. Furthering the body of fundamental knowledge related to polymer composites is crucial for the development of more advanced materials. For example, the overall properties of a polymer composite material are affected by the polymer matrix's interactions with fiber reinforcement or other additives. A region is formed around the fiber or additive known as the "interphase," and the interphase region of the matrix exhibits properties that differ from the bulk properties of the matrix.[2] Specifically, the interphase region can serve as a point of weakness for polymer composite materials. Fiber reinforcement and other additives are used to modify the properties of polymer matrix materials, but it is

necessary to determine how additive presence and interphase presence individually affect material properties.

The present work investigates a novel model system to study the formation of the interphase region and the region's effect on highly crosslinked polymer matrix properties. The model system involves the dispersion of selfsame epoxide-amine microparticles into a highly crosslinked polymer matrix. Specifically, the selfsame microparticles have the same chemical composition as the highly crosslinked polymer matrix into which they are dispersed. Crosslink density's effect on thermomechanical properties has not been investigated for selfsame microparticle systems. Additionally, the impact that selfsame microparticles have on matrix crosslink density has not been investigated. Thus, the present work serves to analyze how the model system is affected by crosslink density, and it also serves to investigate the effect that selfsame microparticle presence has on matrix crosslink density.

Chapter 2: Literature Review

2.1 Highly Crosslinked Polymer Networks

In a fiber-reinforced composite material, the matrix serves to bind the fibers together, transfer mechanical loads between fibers, and protect the fibers from environmental damage.[1] Matrix materials often consist of thermosetting epoxide-amine, polyester, or vinyl ester formulations. Epoxide-amine formulations are prominently used for aerospace-grade composites. The wide variety of available epoxide and amine monomers provides the ability to tailor the network's properties through differences in monomer structure.[1] The reaction of the amine and epoxide functional groups leads to a highly crosslinked structure, which contributes to the mechanical strength, thermal

stability, and environmental stability.[1] Figure 1 depicts the structures of diglycidyl ether of bisphenol-A (DGEBA), triglycidyl-p-aminophenol (p-TGAP), and tetraglycidyl-4,4'-diaminodiphenylmethane (TGDDM), which are examples of epoxide monomers that will respectively form highly crosslinked networks when reacted with an amine monomer such as isophorone diamine (IPDA).

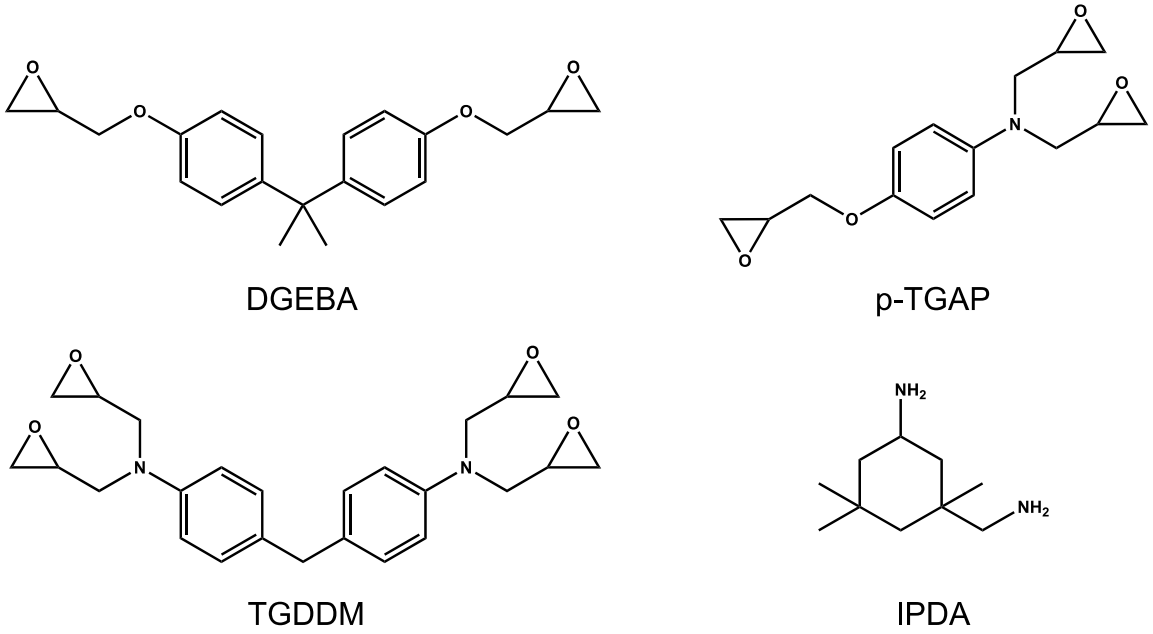

Figure 1. Structures of DGEBA, p-TGAP, TGDDM, and IPDA.

The thermomechanical properties of highly crosslinked polymer networks are typically studied. Analyses are often performed to determine the network's glass transition temperature, which can be obtained through dynamic mechanical analysis (DMA). The analysis can be performed as a function of either temperature or frequency.[3] Because polymeric materials are viscoelastic, they exhibit a delayed response to sinusoidally applied stress. During a DMA experiment, a polymeric material's response to a sinusoidally applied stress is studied, and the material's viscous and elastic behavior

are respectively quantified as the loss modulus and the storage modulus. The ratio of the loss modulus to the storage modulus is known as the tanδ.[3]

The degree of conversion for a highly crosslinked epoxide-amine network is also typically studied, and it can be investigated using Fourier transform near-infrared (FT-NIR) spectroscopy. The disappearance of the epoxide peak at 4530 cm^{-1} can be monitored by comparing a cured network to the corresponding mixture of unreacted monomers.[4] Additionally, the disappearance of the peak can be monitored during the curing reaction through real-time FT-NIR spectroscopy experiments.

2.2 Crosslink Density

Crosslink density describes the degree to which a polymer network is connected in a given volume. Crosslink density affects both the thermal and mechanical properties of a polymer network because the structure of a network largely dictates its material properties.[5] Increasing crosslink density consequently increases the network's structural rigidity, which affects the network's response to mechanical loads and heat. For example, the stiffness of a crosslinked network increases with network rigidity, which is why highly crosslinked materials are characteristically brittle materials. Similarly, increasing a network's crosslink density can result in an increased glass transition temperature, which indicates an increase in the heat required to reach the rubbery state.[5]

In an epoxide-amine network prepared with a 1:1 stoichiometric ratio of reactive epoxide groups to amine protons, the crosslink density is affected by the monomers' structures and the conversion of the network. Monomer structure affects crosslink density mainly through the functionality and the molecular weight between crosslinks.[2] For example, decreasing the molecular weight between crosslinks or increasing monomer

functionality would result in an increased crosslink density.[2,6,7] Systematically changing either of the two parameters can be difficult without introducing other structural features that adversely affect network behavior.[2,8] Alternatively, the conversion of the network can be changed to vary crosslink density. However, the appropriate methods of measuring crosslink density become limited to those that will not affect network conversion.[9] Because of the different variables that can affect crosslink density, it is important to carefully consider the method of varying and measuring crosslink density.

Methods of varying crosslink density dictate what methods are appropriate for quantifying crosslink density. For example, one method involves performing DMA to measure the storage modulus in the rubbery plateau, which is where the storage modulus plateaus above the glass transition temperature. The storage modulus value in the rubbery plateau is then used to calculate crosslink density.[9] Since the method requires that a network is heated beyond the ultimate glass transition temperature, it is not appropriate for measuring the crosslink density of under-cured networks, so it would not be suitable for experiments in which conversion is used to vary crosslink density.[9] However, the method is ideal for the variation of crosslink density through monomer functionality.

2.3 Additives for Highly Crosslinked Polymer Materials

Additives such as nanoparticles and microparticles can be used to modify the thermal and mechanical properties of crosslinked polymer matrix materials. Nanoparticles are additives such as carbon nanotubes and carbon black.[10] Examples of microparticles include crosslinked epoxide-amine microparticles and hollow glass microspheres.[11–13] For epoxide-amine matrix materials, the incorporation of

nanoparticles or microparticles can lead to improved thermal or mechanical properties.[10–12] For example, it is desirable to improve the fracture toughness of the matrix-rich regions in a laminated CFRP composite material, which is especially important for the matrix-rich interlaminar region between layers of carbon fiber. Carbon nanotubes incorporated in the interlaminar region can lead to the improvement of interlaminar fracture toughness.[14]

Crosslinked epoxide-amine microparticles can be prepared via precipitation polymerization.[11] In precipitation polymerization, the epoxide and amine monomers are first solubilized in a solvent such as polypropylene glycol.[11] The monomers react in the initially homogeneous mixture, and when conversion becomes sufficiently high, phase separation occurs as the oligomers become insoluble. The growing epoxide-amine polymers continue to react after precipitation, and the formation of spherical epoxide-amine microparticles occurs.[11] After the microparticles are cured, they are removed from the solvent.

Wu and coworkers prepared crosslinked epoxide-amine microparticles composed of triglycidyl *p*-aminophenol and diethyltoluenediamine via precipitation polymerization in polypropylene glycol.[11] The microparticles were dispersed into an epoxide-amine matrix consisting of diglycidyl ether of bisphenol-A and 4,4'-diaminodiphenylsulfone. For the system studied by Wu and coworkers, dispersing epoxide-amine microparticles into a crosslinked epoxide-amine matrix leads to improved T_g and toughness when compared to the unmodified matrix, and the percent by weight (WT%) of microparticles in the matrix influences the relative improvement in properties. For example, matrix

materials that contain 5 WT% loading of microparticles exhibit the greatest increase in glass transition temperature and network homogeneity.[11]

2.4 The Interphase in Highly Crosslinked Polymer Networks

In polymer composite materials, the matrix surrounding carbon fiber reinforcement or additives such as carbon nanotubes can exhibit properties that differ from the bulk matrix properties.[2,15] The region is known as the interphase, and the dissimilarity in properties is attributed to the additive-matrix interfacial interactions. In an epoxide-amine system, one of the monomers interacting more favorably with the fiber or additive surface can lead to localized stoichiometric imbalances, which impact matrix properties such as glass transition temperature.[15] The interphase region is reported to affect overall material properties, and it has been studied for epoxide-amine matrixes containing additives such as carbon nanotubes and hollow glass microspheres.[2,13]

Improvement of matrix-additive interfacial interactions has been shown to alleviate the effect of a poor interphase region. Incorporating functional groups, which can react with the matrix during the curing process, onto the surface of an additive is a method reported to improve matrix-additive interfacial interactions.[11,16,17] For example, reactive amine functional groups can be used to facilitate covalent bonding between an additive's surface and an epoxide-amine matrix.[16] In the case of epoxide-amine microparticles, the presence of reactive functional groups can be controlled by deviating from a 1:1 stoichiometric ratio during preparation, which can provide epoxide- or amine-functionalized particle surfaces.[11] For epoxide-amine microparticles, Wu and coworkers indicated that reactive functional groups on the surface react with the matrix material during the curing reaction.[11] For the selfsame epoxide-amine microparticle system, the

system's relationship with crosslink density has not been investigated, so it is necessary to first study the relationship without functionalizing the particle surfaces.

Chapter 3: Materials and Methods

3.1 Materials

Diglycidyl ether of bisphenol-A (DGEBA, Hexion EPON 825) with an epoxide equivalent weight (EEW) of 188.5 g/mol, tetraglycidyl-4,4'-diaminodiphenylmethane (TGDDM, Royce International) with an EEW of 112.5 g/mol, and triglycidyl-p-aminophenol (p-TGAP, Huntsman) with an EEW of 100 g/mol were respectively used to prepare epoxide-amine matrix materials. Isophorone diamine (IPDA, Sigma-Aldrich) with an active amine hydrogen equivalent weight of 42.58 g/mol was used as the amine monomer for each system. Polypropylene glycol with M_n = 2000 g/mol (PPG, Sigma-Aldrich) was used to prepare the cured epoxide-amine microparticles. All chemicals were used as received, and no additional purification procedures were employed.

3.2 Preparation of Cured Epoxide-Amine Microparticles

Appropriate amounts of DGEBA, TGDDM, or p-TGAP were respectively mixed with PPG at 50 °C to achieve a homogeneous mixture. Regardless of the epoxide monomer used, the amount of IPDA was selected to achieve a 1:1 stoichiometric ratio of amine and epoxide functional groups. The amount of PPG was selected to make up 60% of the weight of the final mixture, which consisted of the epoxide monomer, IPDA, and PPG. For DGEBA-based microparticles, a representative mixture consisted of DGEBA (0.06491 mol, 24.47 g), IPDA (0.03246 mol, 5.53 g), and PPG (45.00 g). For TGDDM-based microparticles, a representative mixture consisted of TGDDM (0.04836 mol, 21.76 g), IPDA (0.04836 mol, 8.24 g), and PPG (45.00 g). For p-TGAP-based microparticles, a

representative mixture consisted of p-TGAP (0.1403 mol, 42.08 g), IPDA (0.1052 mol, 17.97 g), and PPG (90.00 g). Once the final mixture became homogeneous after continuing to stir at 50 °C, the mixture was transferred to an oven to cure at 100 °C for 24 hours without stirring. After the curing process, the cured microparticles were removed from the PPG via centrifugation in acetone three times, and the acetone was removed by drying under continuous nitrogen flow at 70 °C for 48 hours.

3.3 Neat and 10 WT% Matrix Preparation

Neat matrix materials were prepared by first adding either DGEBA, TGDDM, or p-TGAP to a vacuum filtration flask and stirring under vacuum at 40 °C. Once the bubbling ceased, IPDA was then added to the flask. For each monomer system, a 1:1 stoichiometric ratio was achieved using molar ratios equivalent to those used for the microparticles. The flask contents were subsequently stirred under vacuum at 40 °C, which continued until the mixture was homogeneous and bubbling ceased. The mixture was then poured into a silicone mold which was preheated in an oven at 80 °C. Using the same oven preheated to 80 °C, the material was cured at 80 °C for 2 hours and 150 °C for 2 hours. The microparticle-containing matrix materials were prepared in a similar fashion. However, the materials were prepared with 10 WT% of the selfsame microparticles. For the 10 WT% TGDDM and p-TGAP materials, the microparticles were combined with the IPDA using a sonicating bath. At room temperature, the mixture of IPDA and microparticles was sonicated for 12-15 minutes, which reduced the presence of large agglomerates. Due to the high solid-to-liquid ratio for the microparticle and IPDA mixture, sonicating the particles in the IPDA was not suitable for the DGEBA system. When preparing the 10 WT% DGEBA material, the microparticles were

incorporated by mixing the DGEBA with 15-20 mL of acetone in a vacuum filtration flask at room temperature, which decreased both the mixture's viscosity and the solid-to-liquid ratio. The particles were stirred into the mixture, and the mixture was sonicated at room temperature for 12 minutes to reduce the presence of large agglomerates. The acetone was removed from the mixture by stirring under vacuum at 40 °C until bubbling ceased. After degassing, attenuated total reflectance Fourier transform infrared (ATR-FTIR) spectroscopy was conducted on an aliquot of the mixture to confirm the removal of acetone. Using a range of 600 – 4000 cm^{-1} for a total of 32 scans, the analysis was performed using a ThermoFisher Nicolet 6700 FT-IR spectrometer, which was equipped with a diamond ATR crystal. As depicted in Figure 2, the lack of a significant carbonyl band from 1700 – 1800 cm^{-1} confirmed the removal of acetone.[18] After removing the acetone, the IPDA was added, and the material was degassed and cured as outlined above.

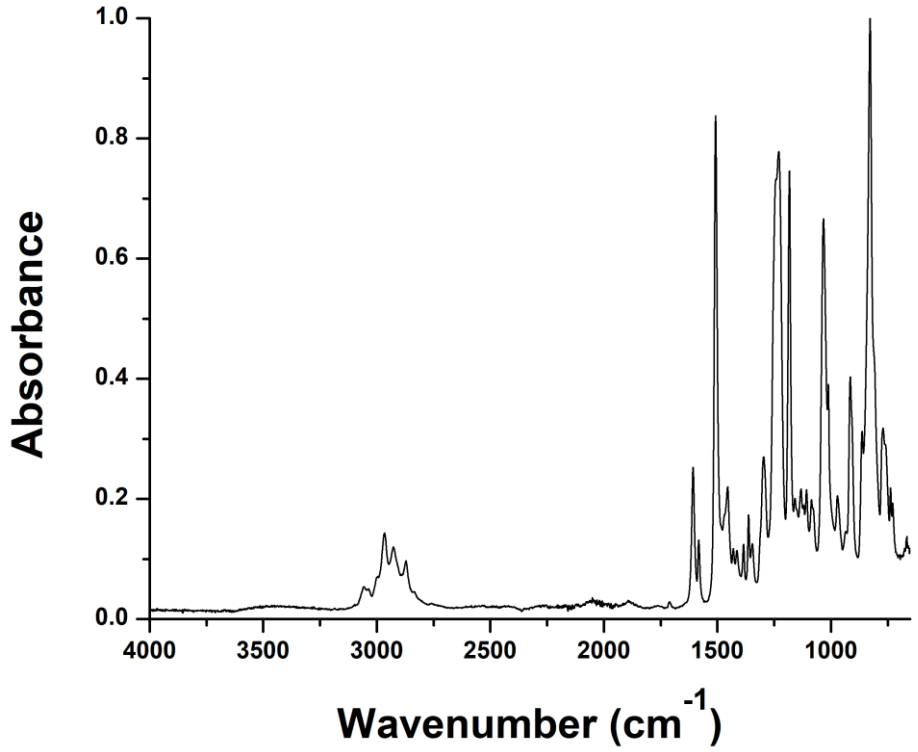

Figure 2. ATR-FTIR spectra of the DGEBA and selfsame microparticle mixture.

3.4 Dynamic Mechanical Analysis (DMA)

Dynamic mechanical analysis (DMA) was conducted using a TA Instruments Q800 Dynamic Mechanical Analyzer. Each experiment was performed using a constant frequency of 1 Hz and a ramp rate of 2 °C/minute. The temperature was ramped from 30 – 300 °C for all samples. Each experiment was run three times to ensure repeatability. The glass transition temperature (T_g) and the storage modulus 30 °C above the T_g were determined using the TA Universal Analysis software package. The temperature corresponding to the peak tanδ value was used as the T_g, and the full width at half maximum (FWHM) was recorded as a measure of network homogeneity. The storage modulus 30 °C above the T_g was used for the determination of crosslink density.

Crosslink density was determined using the method outlined by Hill and coworkers. The method involves the equation $\nu_c = E'/3RT$, where ν_c is crosslink density, E' is storage modulus, R is 8.314 J/K•mol, and T is temperature corresponding to storage modulus.[9]

3.5 Fourier Transform Near-Infrared (FT-NIR) Spectroscopy

For FT-NIR spectroscopy, uncured and cured samples were analyzed using a Perkin Elmer Frontier FTIR. Experiments for all of the uncured and cured samples consisted of 16 scans in transmission over a range of 4000 – 8000 cm^{-1}. The uncured samples were prepared in 20 mL scintillation vials, and the employed molar ratios were identical to those used for the cured samples. For all of the uncured samples, the IPDA was added and thoroughly stirred into the mixture, and a thin layer of the material was spread onto a NIR-transparent glass substrate. For the analysis of the cured materials, the DMA specimens prepared using the cure procedure described in Chapter 3.3 were placed in the beam path.

The degree of conversion (DOC) for each system was calculated by comparing the area of the epoxide peak at 4530 cm^{-1} in the uncured and cured samples. The aromatic hydrogen peak at 4060 cm^{-1} was used as a reference for normalization, and the area of both the epoxide peak and the reference peak were calculated using linear baseline integration in MATLAB. For each spectrum, the area of the peak at 4530 cm^{-1} was normalized to the area of the peak at 4060 cm^{-1}, which gave the normalized area of the epoxide peak for both the uncured ($A_{uncured}$) and cured (A_{cured}) samples. The normalized peak areas were used to calculate DOC using the formula $DOC = 100 \times [1 - (A_{cured})/(A_{uncured})]$.[4]

Chapter 4: Results and Discussion

4.1 Optical Microscopy of Microparticles

After separating the particles from the PPG, optical microscopy was utilized to confirm particle geometry. For each monomer system, images of the microparticles are depicted in Figure 3, and the images illustrate the spherical geometry provided by precipitation polymerization. Between each monomer system, the size and shape of the microparticles did not change significantly.

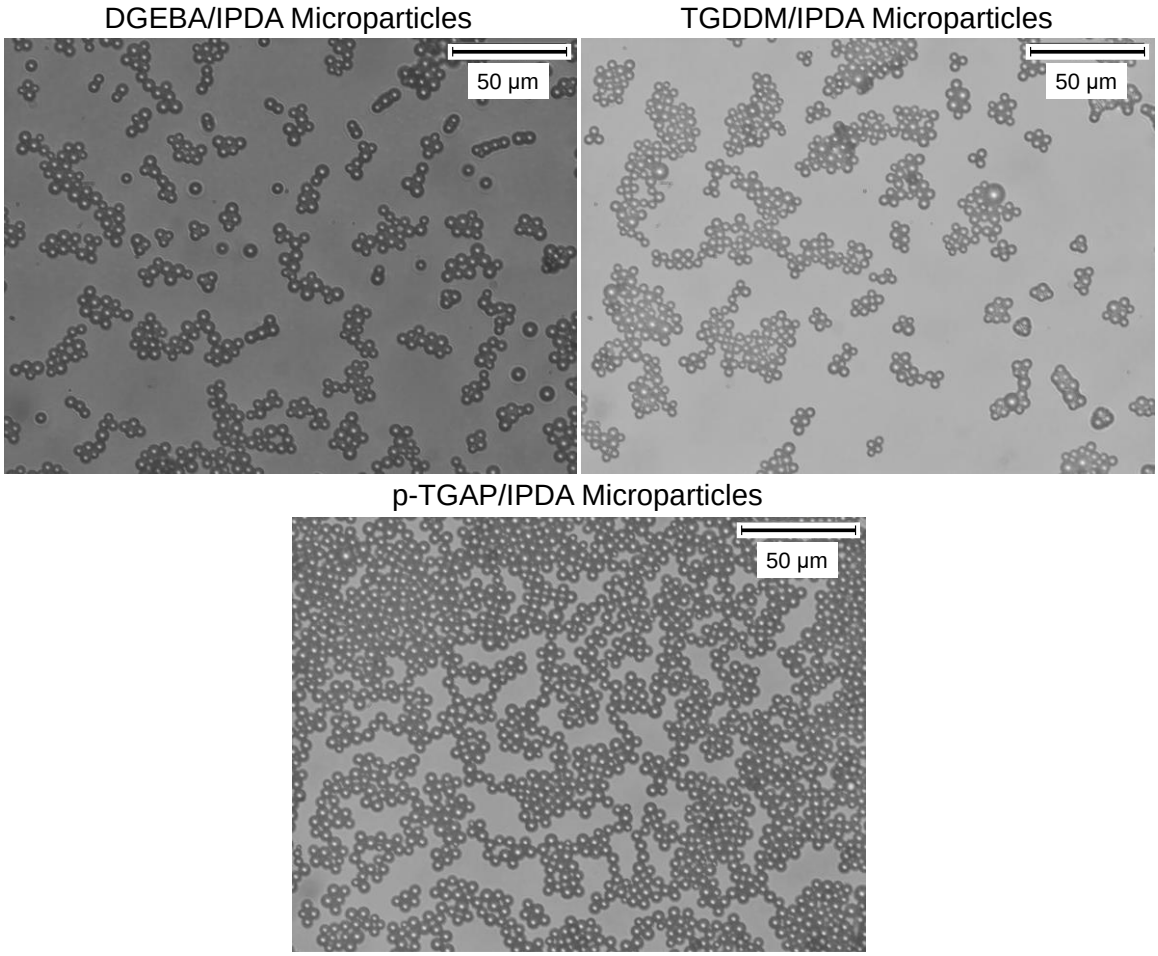

Figure 3. Optical microscopy images of epoxide-amine microparticles.

4.2 Dynamic Mechanical Analysis

Thermomechanical properties of neat and particle-containing materials were investigated via DMA, and representative DMA plots for each of the materials are depicted in Figure 4.

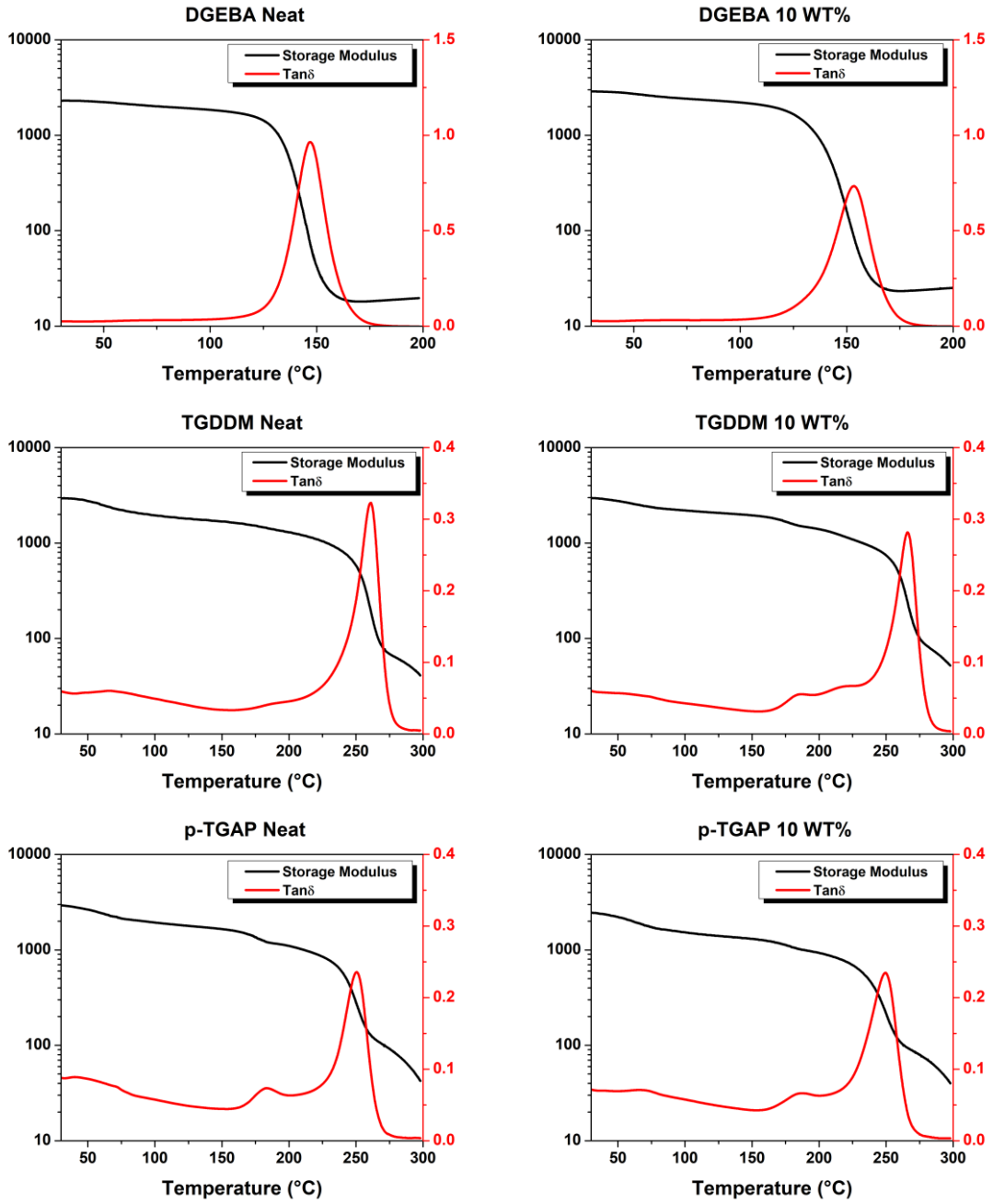

Figure 4. Representative DMA plots for each monomer system.

Table 1. T_g and FWHM for the neat and microparticle-containing materials

System	Particle Loading	T_g (°C)	Standard Deviation T_g (°C)	FWHM (°C)	Standard Deviation FWHM (°C)
DGEBA/IPDA	Neat	148.77	3.09	17.18	0.24
	10 WT%	153.77	1.86	19.49	0.48
TGDDM/IPDA	Neat	261.07	1.06	21.01	2.05
	10 WT%	268.35	1.79	20.21	0.35
p-TGAP/IPDA	Neat	250.21	2.41	21.78	1.13
	10 WT%	248.61	1.61	25.21	0.93

For each monomer system, the T_g and FWHM were obtained through DMA for both the neat and microparticle-containing materials, and the results are reported in Table 1. The inclusion of the microparticles in the TGDDM system led to a slight increase in T_g of 7 °C, which was the greatest change observed for the three monomer systems. The selfsame microparticles led to a minor 5 °C increase in T_g for the DGEBA system. For the p-TGAP system, the selfsame particles led to a decrease in T_g less than 2 °C, and the change is considered insignificant because it falls within the uncertainty of the neat material's T_g.

The FWHM was used to indicate changes in network homogeneity according to microparticle presence. Increased FWHM is associated with a decrease in network homogeneity and vice versa.[11] For the TGDDM system, the observed change in FWHM was within the uncertainty of the neat material's FWHM, which indicated no significant change in network homogeneity. An unchanging FWHM indicated that the microparticles were not associated with an interphase region possessing significantly

different properties than the bulk network. With the presence of microparticles, the FWHM for the DGEBA and p-TGAP systems respectively increased by 2 °C and 3 °C, which indicated slight decreases in network homogeneity. Interphase regions with different properties from the bulk network are concluded to have contributed to the decreased network homogeneity.

For the DGEBA and p-TGAP systems respectively, the minor decreases in network homogeneity are attributed to the effect of tertiary amine presence during the polymerization. The molecular structures of DGEBA, p-TGAP, and TGDDM respectively contain zero, one, and two tertiary amines, which are known to catalyze curing reactions for epoxide-amine networks.[19] Regardless of tertiary amine presence in the epoxide monomer structure, the moiety became increasingly prominent as the primary amines from IPDA were converted to tertiary amines during polymerization. For the investigated systems, the cured microparticles are believed to have introduced tertiary amines that catalyzed the curing reactions near the particle surface. For the DGEBA and p-TGAP systems, the introduction of the cured microparticles is believed to create a disparity between the rates of reaction at the particle surface and in the bulk, and the disparity is attributed to the observed changes in network homogeneity. Although the values depict a greater decrease in network homogeneity for the p-TGAP system, a greater decrease for the DGEBA system is within the uncertainty of the values, and it could be confirmed through additional experiments. Because the molecular structure of TGDDM contains two tertiary amines, the disparity is believed to be the least prominent for the system, which is supported by the relatively unchanged network homogeneity. Thus, tertiary amine presence should be uniform to prevent the formation of a poor

interphase. In conclusion, initial tertiary amine presence is thought to have a significant impact on the observed changes in T_g and FWHM, so the impact of crosslink density cannot be isolated.

The crosslink density was calculated using the method outlined in Chapter 3.4, and the values are reported in Table 2 for each of the neat materials. Because the materials were heated during the analysis, the crosslink density results are indicative of the networks when fully cured. Only a single crosslink density value was obtained for the 10 WT% microparticle TGDDM material because a temperature 30 °C above T_g was not reached during the second and third DMA experiments. Increasing the experimental temperature range would have led to thermal degradation of the material.

Table 2. Crosslink density for each material

System	Particle Loading	Crosslink Density ($mol \cdot m^{-3}$)	Standard Deviation ($mol \cdot m^{-3}$)
DGEBA/IPDA	Neat	1633.18	93.26
	10 WT%	2067.10	36.58
TGDDM/IPDA	Neat	3591.05	108.30
	10 WT%	3874.54	N/A[a]
p-TGAP/IPDA	Neat	5560.23	447.15
	10 WT%	5686.57	695.56

[a]Standard deviation not available, only one value was obtained.

As depicted in Table 2, the neat TGDDM and neat p-TGAP networks respectively had crosslink densities that were approximately 120% and 240% greater than that of the neat DGEBA network. The results illustrated that the crosslink density did not solely

depend on the epoxide monomer's functionality, which is why the neat p-TGAP network had the highest crosslink density without having the highest functionality of the epoxide monomer. The neat p-TGAP network having the highest crosslink density is attributed to the structure of p-TGAP containing a single aromatic ring. The structures of TGDDM and DGEBA both contain two aromatic rings, and the lack of a second ring in p-TGAP provides a lower molecular weight between crosslinks when compared to the other epoxide monomers.

The incorporation of microparticles led to different changes in crosslink density for each of the systems. The DGEBA system demonstrated the most prominent change in crosslink density, and the values were associated with the smallest range of uncertainty. For the p-TGAP system, the crosslink density values were associated with a broad range of uncertainty, and for the TGDDM system, only one crosslink density value was obtained for the 10 WT% material. For the p-TGAP and TGDDM systems respectively, it is difficult to conclude about the effect of microparticle presence on crosslink density. However, increases in crosslink density are accompanied by decreases in tanδ peak amplitude and vice versa.[20] For the present system, the observed changes in tanδ peak amplitude may be used to infer about the changes in crosslink density. When comparing the crosslink density values listed in Table 2 and the tanδ curves depicted in Figure 5, the peak amplitude decreases with increasing crosslink density.

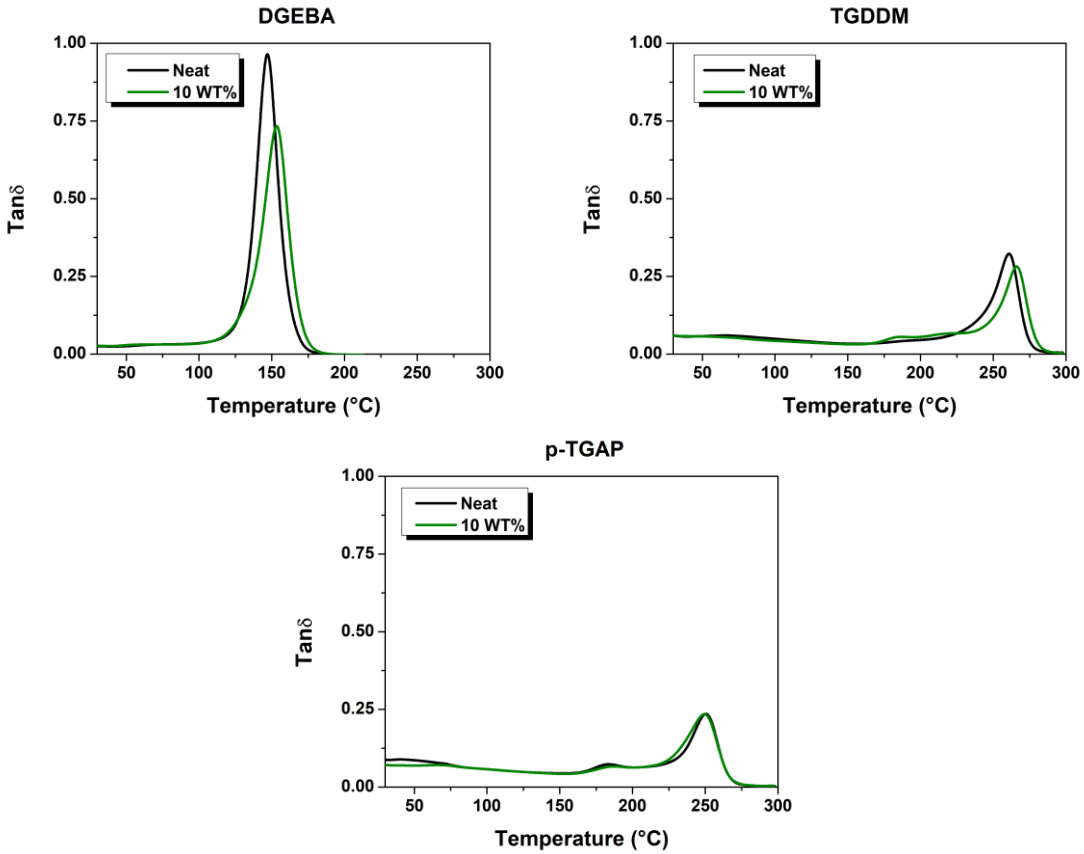

Figure 5. Representative tanδ curves for each monomer system.

The representative tanδ curves in Figure 5 also illustrate the observed effect of particle presence on tanδ peak amplitude. For the DGEBA system, the incorporation of microparticles led to a notable increase in crosslink density, and when compared to the other systems, the most significant decrease in tanδ peak amplitude was observed. The crosslink density values did not change significantly for the p-TGAP system, which is similar to the lack of a change in tanδ peak amplitude. For the p-TGAP system, it is concluded that the crosslink density was not significantly affected by particle presence, which could be confirmed through additional dynamic mechanical analysis experiments. For the 10WT% TGDDM material, the single crosslink density value indicates an increase in crosslink density with particle presence. For the TGDDM system, the

decrease in tanδ peak amplitude supports an increase in crosslink density, but the decrease was less significant than what was observed for the DGEBA system. The crosslink density of the TGDDM system is concluded to have increased when the microparticles were introduced. However, the increase in crosslink density is concluded to be less significant than it was for the DGEBA system. Overall, the results indicate that the microparticles have a greater impact on crosslink density when the neat matrix crosslink density is lower.

4.3 Fourier Transform Near Infrared (FT-NIR) Spectroscopy

The effect of microparticle presence on the degree of conversion (DOC) for each of the monomer systems was studied using Fourier transform near-infrared (FT-NIR) spectroscopy. Using the FT-NIR data plotted in , the DOC was determined using the method outlined in Chapter 3.5, and the results are reported in

Table 3.

Table 3. Degree of conversion for each monomer system

	Degree of Conversion (%)	
System	Neat	10 WT%
DGEBA/IPDA	82.74	81.21
TGDDM/IPDA	86.72	86.99
p-TGAP/IPDA	85.52	89.16

In general, the results indicated that the cured samples were not at full conversion. The TGDDM and p-TGAP networks did not achieve full conversion likely due to the distance between unreacted epoxide and amine groups at high conversion. However, the phenomenon is believed to be more prominent for the DGEBA system, which is why the DGEBA materials had the lowest DOC values. The molecular structures of TGDDM and p-TGAP contain epoxide groups with a shorter distance between them than DGEBA, and as a result, the corresponding networks could achieve a higher conversion before epoxide and amine groups became too separated to react appreciably. The conclusion is

supported by the representative tanδ curves in Figure 5 in Chapter 4.2. For the TGDDM and p-TGAP systems, small peaks were observed between the curing temperature (150 °C) and the T_g. The peaks indicate the occurrence of additional curing reactions during the DMA experiments, so heating the cured TGDDM and p-TGAP materials above the curing temperature would have led to higher conversions than the values obtained through FT-NIR. For the DGEBA system, the T_g is approximately equal to the curing temperature, so it is unlikely that additional curing reactions occurred appreciably.

For each monomer system, the DOC did not change significantly with the incorporation of the microparticles. Thus, the FT-NIR spectroscopy experiments confirmed that the DOC was not significantly affected by selfsame microparticle presence. However, a more in-depth analysis could be conducted using real-time FT-NIR. Real-time FT-NIR could indicate whether tertiary amines on the particle surfaces affect the rate of epoxide disappearance.

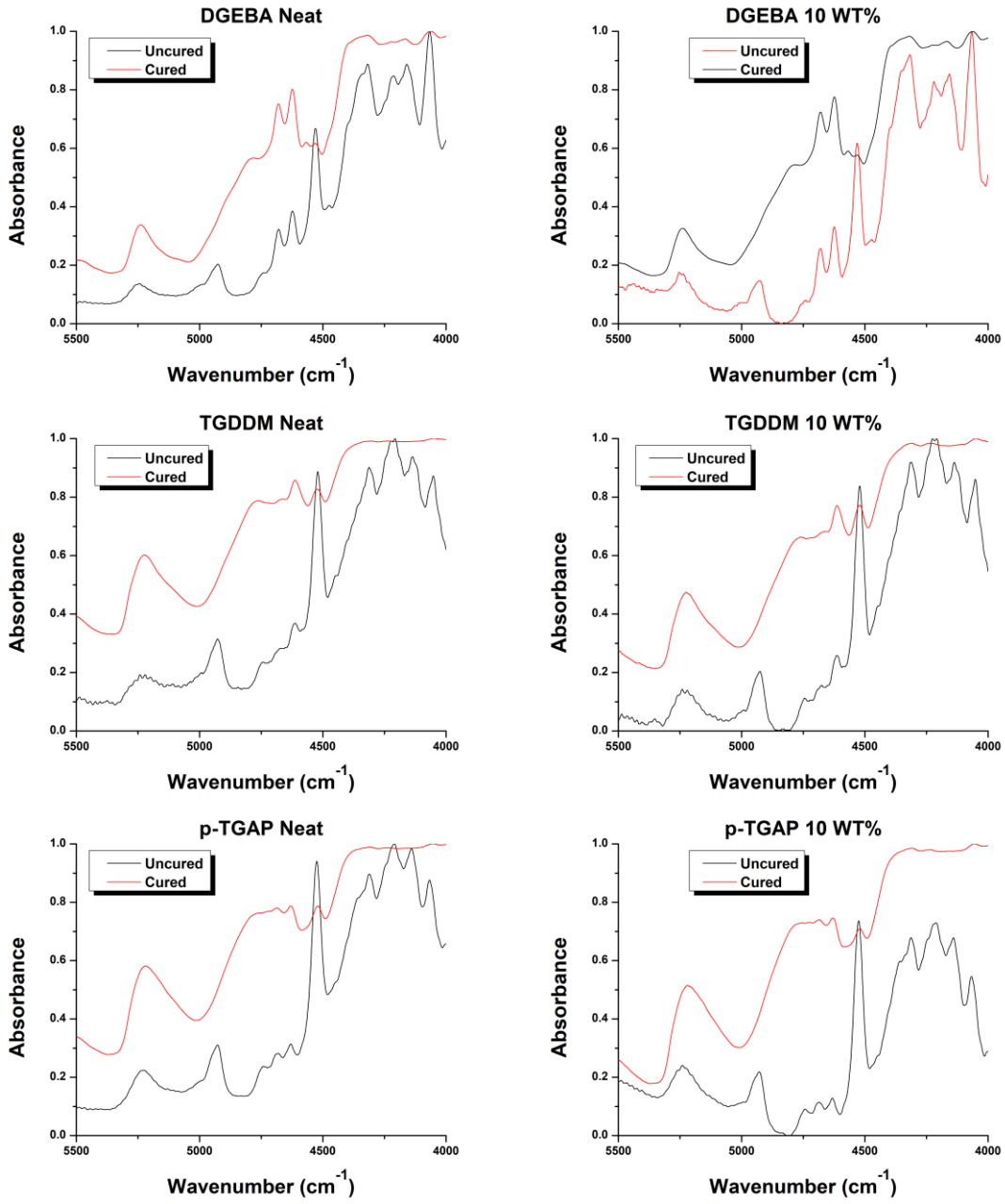

Figure 6. Fourier transform near-infrared spectroscopy data used to monitor the epoxide peak at 4530 cm-1.

Chapter 5: Conclusions

For the investigated epoxide-amine monomer systems, the incorporation of selfsame microparticles led to slightly changed or unchanged glass transition temperatures (T_g) and network homogeneity. The differences in epoxide monomer structures are believed to have impacted the formation of the networks because of the differences in initial tertiary amine presence. Upon the incorporation of microparticles, the T_g increased the most for the system in which tertiary amines were most prevalent in the epoxide monomer structure. For the same system, the network homogeneity was unchanged by the introduction of the microparticles. For the other systems, microparticle presence did not lead to similar increases in T_g, and the network homogeneity was decreased. In conclusion, the initial distribution of tertiary amines in the system is believed to dictate both the properties of the interphase and the observed changes in thermomechanical properties. The effect of microparticle presence on matrix crosslink density was concluded to depend on the crosslink density of the neat matrix material. With the incorporation of selfsame microparticles, the neat matrix material with the lowest crosslink density exhibited the greatest increase in crosslink density. The neat matrix material with the greatest crosslink density exhibited no change in crosslink density when microparticles were introduced. For all of the systems, the microparticles did not lead to significant changes in the degree of conversion. However, the presence of tertiary amines on the microparticle surfaces is thought to affect the rate of epoxide disappearance, and it is hypothesized that the effect would be most prominent at the start of the reaction.

Chapter 6: Future Work

For the selfsame epoxide-amine microparticle system, further investigation of the system's relationship with crosslink density could involve more extensive analysis of crosslink density, degree of conversion, and thermomechanical properties. Further experiments could be conducted to confirm the present conclusions through dynamic mechanical analysis. Additionally, future work could isolate the effect of crosslink density by varying the parameter without inducing significant changes in initial tertiary amine presence, and both higher and lower crosslink densities than the present systems could be studied. Degree of conversion (DOC) could be studied using differential scanning calorimetry (DSC), and the results could be compared to the DOC found through Fourier transform near-infrared (FT-NIR) spectroscopy. Additionally, real-time FT-NIR spectroscopy experiments could be performed to investigate the impact of particle presence on the rate of epoxide disappearance, which could confirm the conclusions about how network homogeneity is affected by tertiary amine presence. The glass transition temperature (T_g) of the microparticles could be obtained using DSC and compared to the T_g of the neat and microparticle-containing matrix materials. Also, the effect of particle presence on the tensile, compressive, and other mechanical properties could be determined for different crosslink densities. Studying the mechanical properties would require a suitable method for measuring the crosslink density of networks at less than full conversion. Alternatively, a post-cure procedure could be employed to achieve full network conversion, and the mechanical properties of the resulting samples could be related to the crosslink density measured at full conversion.

References

(1) Mallick, P. K. *Fiber-Reinforced Composites: Materials, Manufacturing, and Design*, 3rd ed., [expanded and rev. ed.].; CRC Press: Boca Raton, FL, 2008.

(2) Putz, K. W.; Palmeri, M. J.; Cohn, R. B.; Andrews, R.; Brinson, L. C. Effect of Cross-Link Density on Interphase Creation in Polymer Nanocomposites. *Macromolecules* **2008**, *41* (18), 6752–6756. https://doi.org/10.1021/ma800830p.

(3) Goertzen, W. K.; Kessler, M. R. Dynamic Mechanical Analysis of Carbon/Epoxy Composites for Structural Pipeline Repair. *Compos. Part B Eng.* **2007**, *38* (1), 1–9. https://doi.org/10.1016/j.compositesb.2006.06.002.

(4) Rigail-Cedeño, A.; Sung, C. S. P. Fluorescence and IR Characterization of Epoxy Cured with Aliphatic Amines. *Polymer* **2005**, *46* (22), 9378–9384. https://doi.org/10.1016/j.polymer.2005.04.063.

(5) Varley, R. J.; Hodgkin, J. H.; Simon, G. P. Toughening of Trifunctional Epoxy System. V. Structure–Property Relationships of Neat Resin. *J. Appl. Polym. Sci.* **2000**, *77* (2), 237–248. https://doi.org/10.1002/(SICI)1097-4628(20000711)77:2<237::AID-APP1>3.0.CO;2-5.

(6) Plazek, D. J.; Choy, I. C. The Physical Properties of Bisphenol-a-Based Epoxy Resins during and after Curing. II. Creep Behavior above and below the Glass Transition Temperature. *J. Polym. Sci. Part B Polym. Phys.* **1989**, *27* (2), 307–324. https://doi.org/10.1002/polb.1989.090270207.

(7) Won, Y.; Galy, J.; Gérard, J.-F.; Pascault, J.-P.; Bellenger, V.; Verdu, J. Internal Antiplasticization in Copolymer and Terpolymer Networks Based on Diepoxides,

Diamines and Monoamines. *Polymer* **1990**, *31* (9), 1787–1792. https://doi.org/10.1016/0032-3861(90)90203-B.

(8) Cook, W. D.; Mehrabi, M.; Edward, G. H. Ageing and Yielding in Model Epoxy Thermosets. *Polymer* **1999**, *40* (5), 1209–1218. https://doi.org/10.1016/S0032-3861(98)00343-7.

(9) Hill, L. W. Calculation of Crosslink Density in Short Chain Networks. *Prog. Org. Coat.* **1997**, *31* (3), 235–243. https://doi.org/10.1016/S0300-9440(97)00081-7.

(10) Gojny, F. H.; Wichmann, M. H. G.; Köpke, U.; Fiedler, B.; Schulte, K. Carbon Nanotube-Reinforced Epoxy-Composites: Enhanced Stiffness and Fracture Toughness at Low Nanotube Content. *Compos. Sci. Technol.* **2004**, *64* (15), 2363–2371. https://doi.org/10.1016/j.compscitech.2004.04.002.

(11) Wu, X.; Yang, X.; Yu, R.; Zhao, X.-J.; Zhang, Y.; Huang, W. Highly Crosslinked and Uniform Thermoset Epoxy Microspheres: Preparation and Toughening Study. *Polymer* **2018**, *143*, 145–154. https://doi.org/10.1016/j.polymer.2018.04.011.

(12) Park, S.-J.; Jin, F.-L.; Lee, C. Preparation and Physical Properties of Hollow Glass Microspheres-Reinforced Epoxy Matrix Resins. *Mater. Sci. Eng. A* **2005**, *402* (1), 335–340. https://doi.org/10.1016/j.msea.2005.05.015.

(13) Yung, K. C.; Zhu, B. L.; Yue, T. M.; Xie, C. S. Preparation and Properties of Hollow Glass Microsphere-Filled Epoxy-Matrix Composites. *Compos. Sci. Technol.* **2009**, *69* (2), 260–264. https://doi.org/10.1016/j.compscitech.2008.10.014.

(14) Wicks, S. S.; de Villoria, R. G.; Wardle, B. L. Interlaminar and Intralaminar Reinforcement of Composite Laminates with Aligned Carbon Nanotubes. *Compos.*

Sci. Technol. **2010**, *70* (1), 20–28. https://doi.org/10.1016/j.compscitech.2009.09.001.

(15) Palmese, G. R.; McCullough, R. L. Effect of Epoxy–Amine Stoichiometry on Cured Resin Material Properties. *J. Appl. Polym. Sci.* **1992**, *46* (10), 1863–1873. https://doi.org/10.1002/app.1992.070461018.

(16) Ma, P. C.; Kim, J.-K.; Tang, B. Z. Functionalization of Carbon Nanotubes Using a Silane Coupling Agent. *Carbon* **2006**, *44* (15), 3232–3238. https://doi.org/10.1016/j.carbon.2006.06.032.

(17) Ma, P. C.; Kim, J.-K.; Tang, B. Z. Effects of Silane Functionalization on the Properties of Carbon Nanotube/Epoxy Nanocomposites. *Compos. Sci. Technol.* **2007**, *67* (14), 2965–2972. https://doi.org/10.1016/j.compscitech.2007.05.006.

(18) Wallace, W. E. Infrared Spectra. In *NIST Chemistry WebBook, NIST Standard Reference Database Number 69* [Online]; Linstrom, P. J., Mallard, W. G., Eds.; Gaithersburg MD, 20899. https://webbook.nist.gov/cgi/cbook.cgi?ID=C67641&Type=IR-SPEC (accessed February 26, 2020).

(19) Nikolic, G.; Zlatkovic, S.; Cakic, M.; Cakic, S.; Lacnjevac, C.; Rajic, Z. Fast Fourier Transform IR Characterization of Epoxy GY Systems Crosslinked with Aliphatic and Cycloaliphatic EH Polyamine Adducts. *Sensors* **2010**, *10* (1), 684–696. https://doi.org/10.3390/s100100684.

(20) de Nograro, F. F.; Llano-Ponte, R.; Mondragon, I. Dynamic and Mechanical Properties of Epoxy Networks Obtained with PPO Based Amines/MPDA Mixed

Curing Agents. *Polymer* **1996**, *37* (9), 1589–1600. https://doi.org/10.1016/0032-3861(96)83707-4.